Minimum Safety Factor Control in Tokamaks via Optimal Allocation of Spatially Moving Electron Cyclotron Current Drive*

Sai Tej Paruchuri, Andres Pajares, and Eugenio Schuster

***Abstract*— Tokamaks are torus-shaped devices designed to confine a plasma (ionized gas at around 100 million degrees where fusion reactions can take place) using helical magnetic fields. Such magnetic confinement enables light ions, such as isotopes of hydrogen, to stay confined long enough to undergo a fusion reaction. The pitch of the helical magnetic field in a tokamak is characterized by the safety factor q. The safety factor is closely related to the magnetohydrodynamic stability of the plasma. For instance, instabilities that can degrade or even terminate plasma confinement can occur at spatial locations with rational values of the safety factor q. Thus, actively increasing the minimum magnitude of the safety factor can reduce the occurrence of low-order (low rational q values) instabilities. Non-inductive sources of current like neutral beam injection (NBI) and electron cyclotron current drive (ECCD) are used to control the q-profile. ECCD generates electromagnetic waves to drive current and/or heat the plasma. Mirrors are used to control the spatial region of incidence of the generated electromagnetic waves. In this work, the ECCD mirror's position is treated as a controllable input, and its effects are included in the response model used for control design. A controller based on feedback linearization is proposed to simultaneously allocate the NBI and ECCD powers and the ECCD position to track a target minimum safety factor. The effectiveness of the controller is assessed for a DIII-D tokamak scenario in nonlinear one-dimensional simulations using COTSIM (Control-Oriented Transport SIMulator).**

I. Introduction

A plasma is a state of matter in which the atomic particles are dissociated into positively charged ions and negatively charged electrons. Since particles that make up the plasma are charged, magnetic fields can be used to confine it. A tokamak is a torus-shaped device designed to magnetically confine a plasma at a temperature six times the temperature of the Sun's core [1]. Such high temperatures enable light ions, such as isotopes of hydrogen, to undergo thermonuclear fusion reactions and release energy that can be used to generate electricity. Plasmas inside tokamaks exhibit complex dynamics that are modeled by nonlinear partial differential equations (PDEs).

The magnetic field confining the plasma in a tokamak has two components, namely the toroidal magnetic field $\bar{B}_\phi$ and the poloidal magnetic field $\bar{B}_\theta$ (see Figure 1). The pitch of the resulting helical magnetic field lines is measured by the so-called safety factor q. Research on high-performance operating scenarios for tokamaks, which are characterized by potential high fusion power density and steady-state operation, has shown that the safety factor is not only linked to the performance of the plasma but also to its magnetohydrodynamic (MHD) stability [1]. For instance, instabilities like neoclassical tearing modes (NTMs), which can degrade or even terminate the plasma confinement, can occur at locations where the safety factor has a rational value. Thus, actively increasing the minimum of the safety factor profile, q_{min}, can help reduce the likelihood of instabilities corresponding to low safety factor values.

The active control of the safety factor profile in tokamaks has therefore attracted significant attention in recent years [2], [3], [4], [5], [6], [7], [8]. Ideally, it is desirable to control the safety factor value at all the spatial locations from the magnetic axis to the plasma edge (see Figure 1). The spatial shape of the safety factor defines what is usually referred to as a "profile." The evolution of the safety-factor profile is therefore governed by a nonlinear PDE known as the Magnetic Diffusion Equation (MDE). Due to the finite number of actuators available for control, the shaping of the q-profile is achieved either by regulating its value at a finite number of fixed locations or by controlling a finite number of characteristic modes. Moreover, the q-profile usually needs to be controlled in conjunction with other plasma properties such as the plasma beta β, which is defined as the ratio between kinetic and magnetic pressures and is a metric of plasma performance. This need for integration of multiple control objectives further constrains the actuation capabilities for q-profile control, hence reducing the number of controllable spatial locations [8]. As described above, it is often the case where controlling the minimum value of the safety factor profile becomes the main objective due to MHD stability considerations. Controllers proposed in previous work, which are designed to regulate the safety factor at fixed locations, are useful only for special operating modes where the location of the minimum safety factor is fixed (usually at the magnetic axis). However, this is not, in general, the case and the location of the minimum safety factor varies during operation.

Noninductive actuation like neutral beam injection (NBI) and electron cyclotron current drive (ECCD) are used for q-profile control. As the name suggests, a neutral beam injector injects a stream of high-speed neutral particles into the plasma, both driving current and heating the plasma. ECCD, on the other hand, generates electromagnetic waves whose frequency matches that of the electron cyclotron frequency. The resulting resonance is used to drive current and heat the plasma. Mirrors are used to control the ECCD position

*This material is based upon work supported by the U.S. Department of Energy, Office of Science, Office of Fusion Energy Sciences, under Award Numbers DE-SC0010537 and DE-SC0010661. S.T. Paruchuri (saitejp@lehigh.edu), A. Pajares and E. Schuster are with the Department of Mechanical Engineering and Mechanics, Lehigh University, Bethlehem, PA 18015, USA.

(the spatial region of incidence of the electromagnetic waves generated by ECCD). In previous work [2]-[9], the ECCD position is assumed to be fixed during tokamak operation.

By following the original steps in a very recent work by the authors [9], a controller is proposed in this work to regulate the minimum value of the safety factor at time-varying spatial locations. As a notable difference from previous work, the ECCD central position is considered a controllable variable and is allowed to vary over time. The objective of this work is therefore twofold: first, to develop a control-oriented response model that includes the effect of the ECCD position on the q-profile dynamics and, second, to design a model-based controller for the regulation of the minimum safety factor. To the best of the authors' knowledge, this is the first time that a moving ECCD is considered as an actuator for q-profile control in general and for q_{min} control in particular. While this work focuses on controlling the minimum safety factor, the proposed models and methodologies could be extended to the control of other plasma properties that are responsive to a moving ECCD.

The contributions of this work are as follows. A response model that governs the dynamics of the poloidal flux-gradient θ (closely related to q) at the location of the minimum safety factor is introduced in Section II. The proposed model assumes that the ECCD central position can vary over time. A controller based on feedback linearization of the response model and Lyapunov theory is designed in Section III to track a target value for the minimum safety factor. The controller simultaneously allocates the auxiliary powers (NBI and ECCD powers) and the ECCD central position based on a predefined optimal criterion. The effectiveness of the proposed controller is assessed in Section IV for a DIII-D tokamak [10] scenario in nonlinear one-dimensional simulations using the Control-Oriented Transport SIMulator (COTSIM). Finally, conclusions and possible future work are summarized in Section V.

II. Model for Minimum Safety Factor Dynamics

A. Evolution of the Poloidal Flux Gradient

The helical magnetic field $\bar{B}$ in a tokamak can be decomposed into its toroidal and poloidal components, $\bar{B}_\phi$ and $\bar{B}_\theta$, respectively (refer to Figure 1). The poloidal magnetic flux at point P is defined as $\Psi := \int_{\bar{S}} \bar{B}_\theta \cdot d\bar{S}$, where $\bar{S}$ is the surface perpendicular to the z direction and enclosed by the toroidal ring passing through the point P, as shown in Figure 1. A magnetic flux surface is defined by the set of points with identical value of poloidal magnetic flux Ψ. Under ideal magnetohydrodynamic (MHD) conditions, these magnetic flux surfaces form toroidally nested surfaces as shown in Figure 1. It can be shown using the ideal MHD theory that certain plasma variables, like the safety factor q, remain constant on a magnetic flux surface. Furthermore, it is assumed in this study that plasmas inside tokamaks are axisymmetric. As a result, a single spatial variable, as opposed to three spatial variables, that indexes the nested magnetic surfaces is sufficient to characterize the spatial dependence of the plasma properties. In this work, the

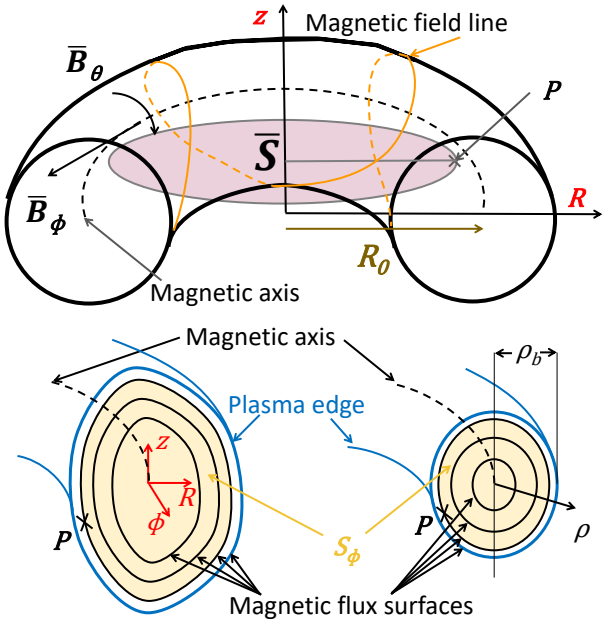

Fig. 1: Magnetic field inside a tokamak.

normalized mean effective minor radius $\hat{\rho} := \frac{\rho}{\rho_b}$ is used as the spatial variable. The variable ρ is the mean effective minor radius and satisfies the relation $\Phi = B_{\phi,0}\pi\rho^2$, where Φ is the toroidal magnetic flux, and $B_{\phi,0}$ is the vacuum toroidal magnetic field at the major radius R_0. The term ρ_b is the value of ρ at the last closed magnetic surface. By definition, the normalized mean effective minor radius takes values in $[0, 1]$. Mathematically, the safety factor at location $\hat{\rho}$ and time t is given by

$$q(\hat{\rho}, t) := -\frac{\partial\Phi/\partial\rho}{2\pi\partial\psi/\partial\rho} = -\frac{B_{\phi,0}\rho_b^2\hat{\rho}}{\partial\psi/\partial\rho}, \tag{1}$$

where $\psi = \Psi/2\pi$ is the poloidal stream function. The minimum safety factor at time t is defined as

$$q_{min}(t) := q(\hat{\rho}_{q_{min}}(t), t), \tag{2}$$

where $\hat{\rho}_{q_{min}}(t) \in [0, 1]$ is equal to the value of $\hat{\rho}$ at which the function $q(\cdot, t)$ takes the minimum value. During tokamak operation, the safety factor profile is computed in real-time. Thus, in this work, the value $\hat{\rho}_{q_{min}}(t)$ at time t is assumed to be computed and available.

The evolution of the poloidal stream function over time is modeled by the magnetic diffusion equation [11]

$$\frac{\partial\psi}{\partial t} = \frac{\eta}{\mu_0\rho_b^2\hat{F}^2}\frac{1}{\hat{\rho}}\frac{\partial}{\partial\hat{\rho}}\left(\hat{\rho}D_\psi\frac{\partial\psi}{\partial\hat{\rho}}\right) + R_0\hat{H}\eta j_{ni} \tag{3}$$

subject to the Neumann boundary conditions

$$\left.\frac{\partial\psi}{\partial\hat{\rho}}\right|_{\hat{\rho}=0} = 0, \qquad \left.\frac{\partial\psi}{\partial\hat{\rho}}\right|_{\hat{\rho}=1} = -\underbrace{\frac{\mu_0}{2\pi}\frac{R_0}{\hat{G}_{\hat{\rho}=1}\hat{H}_{\hat{\rho}=1}}}_{k_{I_p}} I_p. \tag{4}$$

In the above equations, η is the plasma resistivity, j_{ni} is the non-inductive current, μ_0 is the vacuum permeability, and I_p is the plasma current. The terms $\hat{F}, \hat{G}, \hat{H}$ are geometric factors (functions of $\hat{\rho}$) pertaining to the magnetic configuration of a particular MHD equilibrium, and $D_\psi := \hat{F}\hat{G}\hat{H}$.

In this work, control-oriented models developed in [12] are employed to compute the terms η and j_{ni}. The control-oriented model for η is given by

$$\eta \approx g_\eta \times (I_p^\gamma P_{tot}^\epsilon \bar{n}_e^\zeta)^{-3/2}, \tag{5}$$

where g_η is a function of $\hat{\rho}$ that accounts for the spatial variation of the plasma resistivity, P_{tot} is the total injected power, $\bar{n}_e$ is the line-average electron density, and the scaling coefficients γ, ϵ and ζ are constants. On the other hand, the control-oriented model for j_{ni} is such that

$$\begin{aligned}\eta j_{ni} \approx & \sum_{i=1}^{N_{NBI}} g_{NBI,i} \times (I_p^\gamma P_{tot}^\epsilon \bar{n}_e^\zeta)^{(-3/2+\epsilon_{NBI})} \bar{n}_e^{-1} P_{NBI,i} \\ & + g_{EC} \times (I_p^\gamma P_{tot}^\epsilon \bar{n}_e^\zeta)^{(-3/2+\epsilon_{EC})} \bar{n}_e^{-1} P_{EC} \\ & + (\partial\psi/\partial\hat{\rho})^{-1} g_{BS} \times (I_p^\gamma P_{tot}^\epsilon \bar{n}_e^\zeta)^{-1/2} \bar{n}_e,\end{aligned} \tag{6}$$

where $g_{NBI,i}$, g_{EC}, g_{BS} are functions of $\hat{\rho}$ that account for the NBI, EC and bootstrap current depositions, respectively. Note that the EC term g_{EC} corresponds to the (a priori) fixed ECCD position $\bar{\rho}_{ec}$. The efficiency of the NBIs and the ECCD is modeled by the constants ϵ_{NBI} and ϵ_{EC}, respectively. The term N_{NBI} represents the total number of NBI actuators. The terms $P_{NBI,i}$ and P_{EC} are the i^{th} NBI power and EC power, respectively. In the context of this work, these powers are considered the controllable inputs (in addition to the ECCD position, which is discussed in the latter parts of this section). On the other hand, the inputs I_p, $\bar{n}_e$, and P_{tot} are either prescribed as feedforward inputs or determined in real time by competing controllers [8]. The prescribed P_{tot} value will in turn impose a constraint for the q_{min} controller over $P_{NBI,i}$, for $i = 1, \ldots, N_{NBI}$, and P_{EC} since the total injected power P_{tot} is given by $P_{tot} = \sum_{i=1}^{N_{NBI}} P_{NBI,i} + P_{EC}$.

Substituting the expressions (5) and (6) for η and ηj_{ni}, respectively, into (3) and taking the derivative with respect to $\hat{\rho}$ on both sides yields the nonlinear PDE

$$\begin{aligned}\frac{\partial\theta}{\partial t} = & \left(h_{\eta,1}\frac{\partial^2\theta}{\partial\hat{\rho}^2} + h_{\eta,2}\frac{\partial\theta}{\partial\hat{\rho}} + h_{\eta,3}\theta\right)u_\eta + h_{EC}u_{EC} \\ & + \sum_{i=1}^{N_{NBI}} h_{NBI,i}u_{NBI,i} + \left(\frac{h_{BS,1}}{\theta} - h_{BS,2}\frac{\partial\theta/\partial\hat{\rho}}{\theta^2}\right)u_{BS}\end{aligned} \tag{7}$$

subject to the boundary conditions $\theta(0) = 0, \theta(1) = -k_{I_p} I_p$. In the above equations, the term $\theta := \frac{\partial\psi}{\partial\hat{\rho}}$ is the poloidal flux gradient. Note from (1) that the safety factor profile is inversely related to the poloidal flux gradient. Hence, the above dynamical model is used as the basis for safety factor control design. In (7), the terms $h_{\eta,1}, h_{\eta,2}, h_{\eta,3}, h_{EC}, h_{NBI,i}, h_{BS,1}$ and $h_{BS,2}$ are functions of the spatial variable $\hat{\rho}$ and are given by the expressions

$$\begin{aligned}h_{\eta,1} &:= \frac{1}{\mu_0\rho_b^2}\frac{g_\eta}{\hat{F}^2}D_\psi, \\ h_{\eta,2} &:= \frac{1}{\mu_0\rho_b^2}\left[\left(\frac{g_\eta}{\hat{F}^2}\right)' D_\psi + \frac{g_\eta}{\hat{F}^2}\left(\frac{D_\psi}{\hat{\rho}} + 2D'_\psi\right)\right], \\ h_{\eta,3} &:= \frac{1}{\mu_0\rho_b^2}\left[\left(\frac{g_\eta}{\hat{F}^2}\right)'\left(\frac{D_\psi}{\hat{\rho}} + D'_\psi\right) + \frac{g_\eta}{\hat{F}^2}\left(\frac{D'_\psi\hat{\rho} - D_\psi}{\hat{\rho}^2}\right)\right],\end{aligned}$$

$$\begin{aligned}h_{NBI,i} &:= R_0 \times (\hat{H} \times g_{NBI,i})', \qquad h_{EC} := R_0 \times (\hat{H} \times g_{EC})', \\ h_{BS,1} &:= R_0 \times (\hat{H} \times g_{BS})', \qquad h_{BS,2} := R_0 \times \hat{H} \times g_{BS}.\end{aligned} \tag{8}$$

The notation $(\cdot)'$ represents the partial derivative with respect to the spatial variable $\hat{\rho}$. The virtual input terms u_η, $u_{NBI,i}$, u_{EC} and u_{BS} are functions of time and are defined as

$$\begin{aligned}u_\eta &:= (I_p^\gamma P_{tot}^\epsilon \bar{n}_e^\zeta)^{-3/2}, \qquad u_{BS} := (I_p^\gamma P_{tot}^\epsilon \bar{n}_e^\zeta)^{-1/2}\bar{n}_e, \\ u_{NBI,i} &:= (I_p^\gamma P_{tot}^\epsilon \bar{n}_e^\zeta)^{(-3/2+\zeta_{NBI})}\bar{n}_e^{-1}P_{NBI,i}, \\ u_{EC} &:= (I_p^\gamma P_{tot}^\epsilon \bar{n}_e^\zeta)^{(-3/2+\zeta_{EC})}\bar{n}_e^{-1}P_{EC}.\end{aligned}$$

Readers can refer to [8] for the details and intermediate steps involved in deriving (7).

B. Effect of the ECCD Position on the Plasma Dynamics

In the evolution model discussed above, the ECCD position is fixed, i.e., the function g_{EC} that appears in (6) corresponds to the fixed ECCD position $\bar{\rho}_{ec}$. In this case, the value of the function g_{EC} at $\hat{\rho}$ is computed using the control-oriented model [8]

$$g_{EC}(\hat{\rho}) = j_{EC}^{prof}(\hat{\rho})g_\eta(\hat{\rho})\frac{(T_e^{prof}(\hat{\rho})(n_e^{prof}(\hat{\rho}))^\zeta)^{\lambda_{EC}}}{n_e^{prof}(\hat{\rho})}, \tag{9}$$

where j_{EC}^{prof} is the ECCD deposition profile, T_e^{prof} and n_e^{prof} are functions of the spatial variable $\hat{\rho}$, and λ_{EC} is a constant that characterizes the current drive efficiency of the ECCD. In this work, it is assumed that moving the ECCD to a new center $\rho_{ec}(t)$ at time t shifts the entire profile accordingly. Thus, to model the effect of the steering of the ECCD center on j_{EC}^{prof}, a new current deposition profile function $\bar{j}_{EC}^{prof}$ is defined as $\bar{j}_{EC}^{prof}(\rho_{ec}, \hat{\rho}) := j_{EC}^{prof}(\hat{\rho} + \bar{\rho}_{ec} - \rho_{ec})$, where $\rho_{ec} : t \mapsto \rho_{ec}(t)$. Note that $j_{EC}^{prof}(\hat{\rho}) = \bar{j}_{EC}^{prof}(\bar{\rho}_{ec}, \hat{\rho})$. Thus, in the governing equation (7), the function $h_{EC}(\hat{\rho})$ (defined in (8)) is replaced by $\bar{h}_{EC}(\rho_{ec}, \hat{\rho})$, which is given by

$$\bar{h}_{EC}(\rho_{ec}, \hat{\rho}) := R_0 \times (\hat{H}(\hat{\rho})\bar{g}_{EC}(\rho_{ec}, \hat{\rho}))', \tag{10}$$

where

$$\bar{g}_{EC}(\rho_{ec}, \hat{\rho}) := \bar{j}_{EC}^{prof}(\rho_{ec}, \hat{\rho})g_\eta(\hat{\rho})\frac{(T_e^{prof}(\hat{\rho})(n_e^{prof}(\hat{\rho}))^\zeta)^{\lambda_{EC}}}{n_e^{prof}(\hat{\rho})}.$$

It is clear from the definition of $\bar{j}_{EC}^{prof}$ that the value of j_{EC}^{prof} at points outside $[0, 1]$ may sometimes be required. For example, suppose $\bar{\rho}_{ec} = 0$. Then, $\bar{j}_{EC}^{prof}(0, 0.5) = j_{EC}^{prof}(-0.5)$. Experiments show that the effect of the ECCD is highly localized and the function j_{EC}^{prof} has compact support. Thus, it is assumed that the fixed ECCD position $\bar{\rho}_{ec}$ is such that the support of j_{EC}^{prof} is contained in $(0, 1)$. Thus, under this assumption, the value of the function j_{EC}^{prof} at $\hat{\rho} \notin [0, 1]$ can be defined to be equal to zero.

C. Evolution of θ at the Minimum Safety Factor Location

To design a controller that tracks a target minimum safety factor $\bar{q}_{min}$, a model that captures the dynamics of θ explicitly at the location $\hat{\rho}_{q_{min}}$ of the minimum safety factor is required. Recall that $\hat{\rho}_{q_{min}} : t \mapsto \hat{\rho}_{q_{min}}(t)$ maps time t to the location of the minimum safety factor. Substituting $\hat{\rho} = \hat{\rho}_{q_{min}}$ into the governing equation (7) with the term h_{EC}

replaced by $\bar{h}_{EC}(\rho_{ec})$ in (10) reduces the autonomous PDE into a nonautonomous ordinary differential equation (ODE) of the form

$$\begin{aligned}\dot{\theta}_{q_{min}} = &\underbrace{\left(h^{min}_{\eta,1}\theta''_{q_{min}} + h^{min}_{\eta,2}\theta'_{q_{min}} + h^{min}_{\eta,3}\theta_{q_{min}}\right)u_{\eta}}_{c_1} \\ &+ \sum_{i=1}^{N_{NBI}} h^{min}_{NBI,i}u_{NBI,i} + \bar{h}^{min}_{EC}(\rho_{ec})u_{EC} \\ &+ \underbrace{\left(h^{min}_{BS,1}\frac{1}{\theta_{q_{min}}} - h^{min}_{BS,2}\frac{\theta'_{q_{min}}}{\theta^2_{q_{min}}}\right)u_{BS}}_{c_2},\end{aligned} \tag{11}$$

where $\theta_{q_{min}} := \theta(\hat{\rho}_{q_{min}}(\cdot),\cdot)$, $\theta'_{q_{min}} := \theta'(\hat{\rho}_{q_{min}}(\cdot),\cdot)$, $\theta''_{q_{min}} := \theta''(\hat{\rho}_{q_{min}}(\cdot),\cdot)$, $h^{min}_{(\cdot)} := h_{(\cdot)} \circ \hat{\rho}_{q_{min}}$, $\bar{h}^{min}_{EC}(\rho_{ec}) \equiv \bar{h}^{min}_{EC}(\rho_{ec},\cdot) := \bar{h}_{EC}(\rho_{ec},\hat{\rho}_{q_{min}}(\cdot))$. In the above equation, the notation $\dot{(\cdot)}$ denotes the derivative with respect to time t while the notations $(\cdot)'$ and $(\cdot)''$ represent first and second order derivatives with respect to the spatial variable $\hat{\rho}$. Note that the terms $\theta_{q_{min}}, \theta'_{q_{min}}, \theta''_{q_{min}}$, and $h^{min}_{(\cdot)}$ are functions of time t. The term $\bar{h}^{min}_{EC}$, on the other hand, is a function of the controllable variable ρ_{ec} as well as time t.

III. Control Design

In this section, the response model derived above is used to develop a control algorithm. If a target $\bar{q}_{min}$ is given, the target poloidal flux gradient at the minimum safety factor location $\bar{\theta}_{q_{min}}(t)$ at time t is given by

$$\bar{\theta}_{q_{min}}(t) = -\frac{B_{\phi,0}\rho_b^2\hat{\rho}_{q_{min}}(t)}{\bar{q}_{min}(t)}. \tag{12}$$

The objective is to choose the inputs $P_{NBI,i}$, P_{EC} and ρ_{ec} such that the system tracks the target. Suppose that the terms $h^{*,min}_{NBI,i}$ and $\bar{h}^{*,min}_{EC}(\rho_{ec})$ are defined such that $h^{min}_{NBI,i}\ u_{NBI,i} = h^{*,min}_{NBI,i}\ P_{NBI,i}$ and $\bar{h}^{min}_{EC}(\rho_{ec})\ u_{EC} = \bar{h}^{*,min}_{EC}(\rho_{ec})\ P_{EC}$. The tracking is achieved through feedback-linearization, in which the inputs $P_{NBI,i}$, P_{EC} and ρ_{ec} are chosen such that

$$\begin{aligned}\sum_{i=1}^{N_{NBI}} h^{*,min}_{NBI,i}P_{NBI,i} + \bar{h}^{*,min}_{EC}(\rho_{ec})P_{EC} + c_1 + c_2 \\ = -K_p\tilde{\theta}_{q_{min}} - K_I\int_{t_0}^{t}\tilde{\theta}_{q_{min}}dt + \dot{\bar{\theta}}_{q_{min}},\end{aligned} \tag{13}$$

where $K_p > 0$, $K_I > 0$ are controller gains and $\tilde{\theta}_{q_{min}} = \theta_{q_{min}} - \bar{\theta}_{q_{min}}$. From (11), note the definition of c_1 and c_2, it is evident that the LHS of the above equation (13) is equal to $\dot{\theta}_{q_{min}}$. Thus, when the inputs satisfy the above equality, the evolution of the error $\tilde{\theta}$ is governed by

$$\dot{\tilde{\theta}}_{q_{min}} = -K_p\tilde{\theta}_{q_{min}} - K_I\int_{t_0}^{t}\tilde{\theta}_{q_{min}}dt. \tag{14}$$

The asymptotic stability of the above system is proven in [9]. Suppose that the inputs P_{NBI} and P_{EC} have both feedforward and feedback components. That is, $P_{NBI,i} = P_{NBI,ff,i} + P_{NBI,fb,i}$ and $P_{EC} = P_{EC,ff} + P_{EC,fb}$, where the subscripts ff and fb represent the feedforward and feedback terms, respectively. Then, (13) can be rewritten as

$$h^T(\rho_{ec})u_{fb} + b_1(\rho_{ec}) = 0, \tag{15}$$

where

$$\begin{aligned}h(\rho_{ec}) &= \left[h^{*,min}_{NBI,1}, \quad \cdots, \quad h^{*,min}_{NBI,N_{NBI}}, \quad \bar{h}^{*,min}_{EC}(\rho_{ec})\right]^T, \\ b_1 &= K_p\tilde{\theta}_{q_{min}} + K_I\int_{t_0}^{t}\tilde{\theta}_{q_{min}}dt - \hat{c}, \\ \hat{c} &= \dot{\bar{\theta}}_{q_{min}} - c_1 - c_2 - h^T(\rho_{ec})u_{ff}, \\ u_{(\cdot)} &= \left[P_{NBI,(\cdot),1}, \quad \cdots, \quad P_{NBI,(\cdot),N_{NBI}}, \quad P_{EC,(\cdot)}\right]^T.\end{aligned}$$

In addition to the above equation, it is clear from the discussion in Subsection II-A that the inputs must satisfy

$$\mathbb{1}^T u_{fb} + b_2 = 0, \tag{16}$$

where $\mathbb{1} = [1,\ldots,1]^T \in \mathbb{R}^{N_{NBI}+1}$ and $b_2 = -P_{tot} + \mathbb{1}^T u_{ff}$. Since there are $N_{NBI}+2$ control inputs and only two constraints ((15) and (16)), there is no unique way to choose $P_{NBI,fb,i}$, $P_{EC,fb}$ and ρ_{ec}. In this work, these values at each time t are chosen by minimizing a cost function subject to the constraints imposed by (15) and (16). The following subsection focuses on deriving a closed-form expression for the solution of the optimization problem.

A. Statement and Solution of Optimization Problem

The optimization problem at each time t is posed as

$$\underset{u(t),\rho_{ec}(t)}{\operatorname{argmin}}\ f(u(t)) = \underset{u(t),\rho_{ec}(t)}{\operatorname{argmin}}\ u^T(t)Qu(t) \tag{17}$$

subject to the constraints

$$g_1(\rho_{ec}(t),u(t)) := \hat{h}^T(\rho_{ec}(t))u(t) + b_1(\rho_{ec}) = 0, \tag{18}$$

$$g_2(u(t)) := \hat{\mathbb{1}}^T u(t) + b_2 = 0, \tag{19}$$

$$u(t) \in \Gamma \times (-\infty,\infty) \times (-\infty,\infty), \text{ and} \tag{20}$$

$$\rho_{ec} \in [0,1]. \tag{21}$$

In the above equations, $u \triangleq \begin{bmatrix}u_{fb}^T & s_1 & s_2\end{bmatrix}^T$, $\hat{h}(\rho_{ec}) \triangleq \begin{bmatrix}h^T(\rho_{ec}) & 1 & 0\end{bmatrix}^T$, $\hat{\mathbb{1}} \triangleq \begin{bmatrix}\mathbb{1}^T & 0 & 1\end{bmatrix}^T$, where s_1 and s_2 are slack variables introduced to ensure the existence of a solution to the optimization problem even when constraints (15) and (16) cannot be satisfied exactly. The term Q is a diagonal matrix given by $Q = diag(q_1,\ldots,q_{N_{NBI}+1},q_{s_1},q_{s_2})$, $q_{s_1},q_{s_2} >> q_i > 0$ for $i = 1,\ldots,N_{NBI}+1$. The set $\Gamma = [\underline{\gamma}_1,\bar{\gamma}_1] \times \ldots \times [\underline{\gamma}_{N_{NBI}+1},\bar{\gamma}_{N_{NBI}+1}] \subset \mathbb{R}^{N_{NBI}+1}$ accounts for the lower and upper saturation limits associated with the NBI and ECCD powers. Note that the ECCD position term explicitly appears only in the constraint equation and not in the cost function. In the following analysis, the time notation (t) is dropped for convenience.

To simplify the above optimization problem, the optimization problem for a fixed ECCD position $\hat{\rho}_{ec} \in [0,1]$ without actuator saturation limits (20) is first solved. The Lagrange multiplier theorem gives a closed form expression for the solution of this problem. Suppose that $g_1^* := g_1(\hat{\rho}_{ec},\cdot)$, $\hat{h}^* := \hat{h}(\hat{\rho}_{ec})$, $h^* := h(\hat{\rho}_{ec})$ and $b_1^* := b_1(\hat{\rho}_{ec})$. Define the Lagrangian as

$$\mathcal{L}(u,\lambda_1,\lambda_2) = f(u) - \lambda_1 g_1^*(u) - \lambda_2 g_2(u), \tag{22}$$

where $\lambda_1, \lambda_2 \in \mathbb{R}$ are the Lagrange multipliers. The Lagrange multiplier theorem [13] states that if a local minimum u^* exists, and the Jacobian $\begin{bmatrix}\nabla_u g_1^*(u^*) & \nabla_u g_2(u^*)\end{bmatrix}^T$ has rank 2, then there exist λ_1^* and λ_2^* such that $\nabla\mathcal{L}(u^*, \lambda_1^*, \lambda_2^*) = 0$. Solving the equation for u^* results in the expression

$$u^* = \frac{1}{2}Q^{-1}\begin{bmatrix}\hat{h}^* & \hat{\mathbb{1}}\end{bmatrix}\begin{bmatrix}\hat{h}^{*^T}Q^{-1}\hat{h}^* & \hat{h}^{*^T}Q^{-1}\hat{\mathbb{1}} \\ \hat{\mathbb{1}}^T Q^{-1}\hat{h}^* & \hat{\mathbb{1}}Q^{-1}\hat{\mathbb{1}}\end{bmatrix}\begin{bmatrix}-2b_1^* \\ -2b_2\end{bmatrix} \quad (23)$$

Note that the level sets $f(u) = p$, where p is some arbitrary positive constant, form concentric ellipses. Also, the set of points that satisfy both constraints forms a hyperplane. The solution u^* corresponds to the point at which the level set with the least value of p is tangential to the hyperplane. This shows that the above expression for u^* is indeed a minimum.

It is known that if the solution of the optimization problem without saturation constraints is outside the set Γ, the extremum of the same problem with saturation constraints is achieved at the boundary of the set Γ. The following algorithm uses this fact to solve the optimization problem with saturation limits in an iterative manner. The subscript i represents the i^{th} element of a vector.

Algorithm 1: Algorithm for computing the saturated inputs for a given ECCD position.

Inputs: h^*, b_1^*, b_2, Q. *Outputs:* u^*.

1) Set $\tilde{h} = [\ ]$, an empty vector; and calculate u^* using (23).
2) For $i = 1, \ldots, N_{NBI} + 1$,
   - if $u_i <= \underline{\gamma}_i$
     $b_1^* = b_1^* + \underline{\gamma}_i * h_i^*, \qquad b_2 = b_2 + \underline{\gamma}_i$
   - elseif $u_i >= \bar{\gamma}_i$
     $b_1^* = b_1^* + \bar{\gamma}_i * h_i^*, \qquad b_2 = b_2 + \bar{\gamma}_i$
   - else
     $\tilde{h} = [\tilde{h}; h_i^*], \qquad \tilde{q} = [\tilde{q}; q_i]$
3) Set $h^* = \tilde{h}$, $\mathbb{1} = ones(size(\tilde{h}))$, $Q = diag(\tilde{q}, q_{s_1}, q_{s_2})$.
4) If $size(h^*) == 0$,
   stop;
   else,
   return to Step 1.

The next step is to come up with an algorithm that treats the ECCD position as a variable. Before proceeding further, note that during tokamak operation, the maximum allowable change in the ECCD position at every time step is bounded from above by a constant δ. The following algorithm provides a simple solution for solving the nonlinear optimization problem posed at the beginning of this subsection. A finite discrete set of possible ECCD positions at a given time step is first considered. For each value of the ECCD position in the set, Algorithm 1 is implemented. The optimal ECCD position and inputs are the ones that correspond to the least cost value. Similar to the previous algorithm, the subscripts i and j in the following algorithm represents the i^{th} and j^{th} elements of a vector, respectively. Additionally, the superscript k represents the k^{th} time step.

Algorithm 2: Algorithm for optimization problem with moving ECCD.

Inputs: ρ_{ec}^{k-1}. *Outputs:* $u^{*,k}$, $\rho_{ec}^{*,k}$.

1) Define the vector

$$\Omega^k := \begin{cases} [0, \delta] & \text{if } \rho_{ec}^{k-1} = 0, \\ [1-\delta, 1] & \text{if } \rho_{ec}^{k-1} = 1, \\ [\rho_{ec}^{k-1} - \delta, \rho_{ec}^{k-1}, \rho_{ec}^{k-1} + \delta] & \text{otherwise.} \end{cases}$$

   In the above definition, the term ρ_{ec}^{k-1} represents the position of the ECCD at the previous time step.
2) For $i = 1, \ldots,$ length of Ω^k,
   a) Set $\hat{\rho}_{ec}^k = \Omega_i^k$.
   b) Compute inputs $u_i^{*,k}$ with $\hat{\rho}_{ec}^k$ using Algorithm 1. Set $J_i^k = u_i^{*,k^T} Q u_i^{*,k}$.
3) Set j such that $J_j^k = min_i J_i^k$. Set $u^{*,k} = u_j^{*,k}$ and $\rho_{ec}^{*,k} = \Omega_j^k$.

IV. Performance Assessment via Simulation

The above control algorithm was tested in 1D nonlinear simulations using the Control Oriented Transport SIMulation (COTSIM) for the DIII-D tokamak scenario. In the simulations, $N_{NBI} = 2$, $\delta = 0.01$, and $\rho_{ec}^0 = 0.475$ were chosen. The target $\bar{q}_{min}$ was generated using the input data corresponding to the DIII-D shot 147634. The NBI feedforward signals were set equal to those inputs used to generate the target values, while the feedforward EC power were set equal to zero in all the simulations (i.e., $P_{EC,ff} = 0$). The total power P_{tot} was generated using the control algorithm for tracking a target plasma total energy given in [8]. During the simulations, the controller was activated at 2.5 seconds. The grey background in the figures denotes the time interval when the controller is active. The controller gains were chosen as $K_P = 0.03$ and $K_I = 5 \times 10^{-4}$, and the Q matrix in the cost function was selected as $Q = diag(1, 1, 1, 1000, 1000)$. The upper saturation limits of $P_{NBI,1}$, $P_{NBI,2}$ and P_{EC} were 12 MW, 6 MW and 4.5 MW, respectively; whereas the lower saturation limits for all three powers were 0 MW.

To evaluate the difference in performance when the ECCD position is used for control, the control algorithm for the fixed ECCD case (i.e., Algorithm 2 with $\Omega^k = \{\rho_{ec}^{k-1}\}$) is tested along with the moving ECCD case. Figure 2 shows the q_{min} evolution over time for both cases. The figure also shows the ρ_{ec} and $\hat{\rho}_{q_{min}}$ values. The q_{min} starts to diverge from the target after 2 seconds in the absence of feedback. On the other hand, the system under feedback control tracks the given target in both the fixed and moving ECCD cases. It can also be seen that the optimal ECCD position for the moving ECCD case is roughly located at $\hat{\rho}_{q_{min}} + 0.115$. Figure 3 shows how the NBI and ECCD powers change with time when the ECCD position is both fixed and allowed to vary. When the ECCD is fixed $P_{NBI,2}$ saturates approximately from 3.5 to 4 seconds and from 5.25 to 5.75 seconds. The control algorithm compensates for this saturation by causing a significant increase in the ECCD power P_{EC}. Note that there are three actuators and two linear constraints (18)

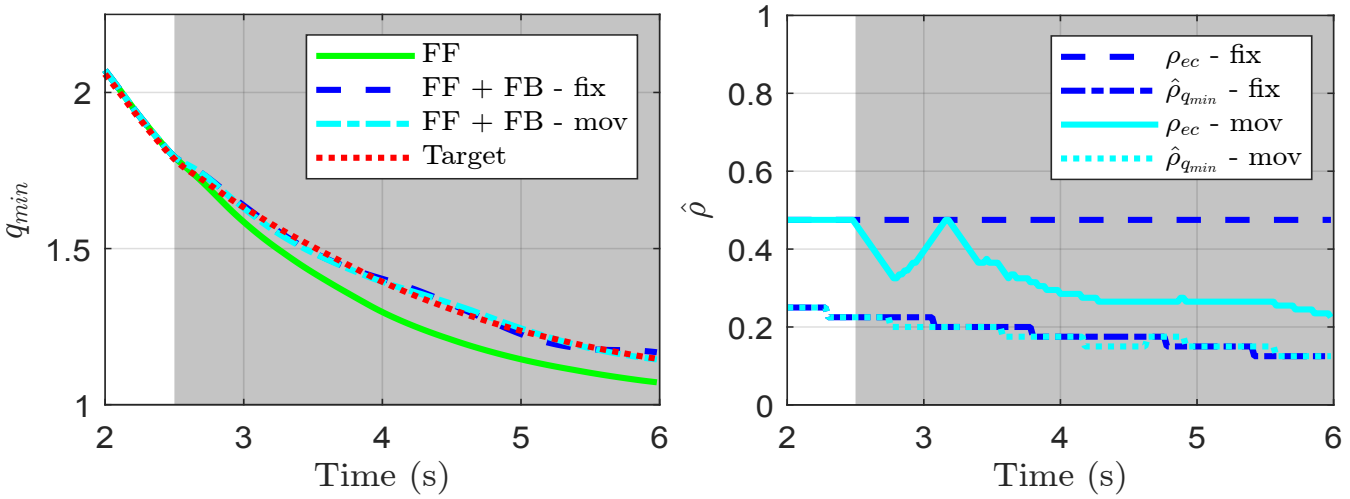

Fig. 2: Fixed and moving ECCD cases: minimum safety factor evolution (left), ECCD position (right).

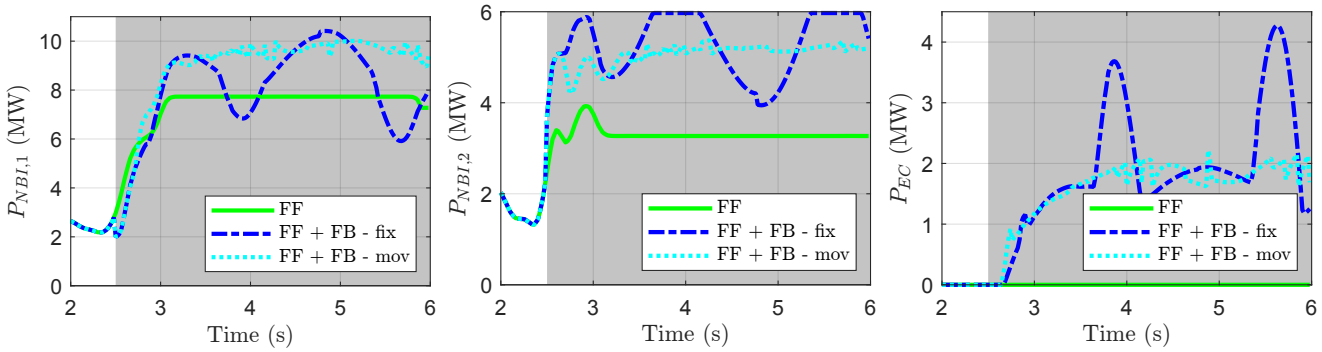

Fig. 3: Fixed and moving ECCD cases: Auxiliary powers - $P_{NBI,1}$ (left), $P_{NBI,2}$ (center), P_{EC} (right)

and (19). The ECCD power P_{EC} increases because there is only a unique choice of $P_{NBI,1}$ and P_{EC} to satisfy both constraints when $P_{NBI,2}$ saturates. In contrast, $P_{NBI,2}$ does not saturate when the ECCD position is allowed to vary. As a result, the controller does not cause any spike in P_{EC}.

V. Conclusion and Future Work

A dynamic model for the poloidal flux gradient θ at the location of the minimum safety factor q_{min} was presented. The model treats the ECCD position as a controllable input. An optimal feedback-linearization-based controller that tracks a target minimum safety factor was also proposed. The effectiveness of the controller was tested in COTSIM simulations for a DIII-D tokamak scenario. This work suggests that treating the ECCD position as a controllable variable can enhance actuation efficiency in q-profile control applications. In particular, simulations in this work show that controlling the ECCD position can prevent actuator saturation and/or a sudden increase in actuator powers. Future work could potentially focus on employing a spatially moving ECCD in other plasma control applications like the regulation of the electron temperature profile.

References

[1] J. Wesson and D. J. Campbell, *Tokamaks*. Oxford university press, 2011, vol. 149.

[2] T. Wijnands *et al.*, "Feedback control of the current profile on Tore Supra," *Nuclear Fusion*, vol. 37, no. 6, pp. 777–791, Jun. 1997.

[3] T. Suzuki *et al.*, "Off-axis current drive and real-time control of current profile in JT-60U," *Nuclear Fusion*, vol. 48, no. 4, p. 045002, Feb. 2008.

[4] D. Moreau *et al.*, "A two-time-scale dynamic-model approach for magnetic and kinetic profile control in advanced tokamak scenarios on JET," *Nuclear Fusion*, vol. 48, no. 10, p. 106001, Aug. 2008.

[5] F. B. Argomedo *et al.*, "Lyapunov-based distributed control of the safety-factor profile in a tokamak plasma," *Nuclear Fusion*, vol. 53, no. 3, p. 033005, Feb. 2013.

[6] J. Barton *et al.*, "Physics-model-based nonlinear actuator trajectory optimization and safety factor profile feedback control for advanced scenario development in DIII-D," *Nuclear Fusion*, vol. 55, no. 9, p. 093005, Jul. 2015.

[7] W. Wehner *et al.*, "Optimal current profile control for enhanced repeatability of L-mode and H-mode discharges in DIII-D," *Fusion Engineering and Design*, vol. 123, pp. 513–517, Nov. 2017.

[8] A. Pajares and E. Schuster, "Current profile and normalized beta control via feedback linearization and lyapunov techniques," *Nuclear Fusion*, vol. 61, no. 3, p. 036006, jan 2021.

[9] ——, "Robust Nonlinear Control of the Minimum Safety Factor in Tokamaks," in *5th IEEE Conference on Control Technology and Applications*, Aug. 2021, in press.

[10] "DIII-D National Fusion Facility," https://www.ga.com/magnetic-fusion/diii-d.

[11] F. L. Hinton and R. D. Hazeltine, "Theory of plasma transport in toroidal confinement systems," *Reviews of Modern Physics*, vol. 48, no. 2, pp. 239–308, Apr. 1976.

[12] J. E. Barton *et al.*, "Physics-based control-oriented modeling of the safety factor profile dynamics in high performance tokamak plasmas," in *52nd IEEE Conference on Decision and Control*, Dec. 2013, pp. 4182–4187.

[13] M. R. Hestenes, "Optimization theory: the finite dimensional case," *New York*, 1975.